Volume and surface area of Holstein dairy cows calculated from complete 3D shapes acquired using a high-precision scanning system: Interest for body weight estimation

Yannick Le Cozler, C. Allain, Caroline Xavier, L. Depuille, Anaïs Caillot, J.M. Delouard, L. Delattre, T. Luginbuhl, Philippe Faverdin

Volume and surface area of Holstein dairy cows calculated from complete 3D shapes acquired using a high-precision scanning system: interest for body weight estimation

Y. Le Cozler[(1)], C Allain[(2)], C Xavier[(1)], L. Depuille[(2)], A. Caillot[(1)], J.M. Delouard[(3)], L. Delattre[(3)], T. Luginbuhl[(3)], P. Faverdin[(1)]*

(1) PEGASE, Agrocampus-Ouest, INRA, 35590 Saint-Gilles, France

(2) Institut de l'Elevage, Monvoisin, 35652 Le Rheu, France

(3) 3D Ouest, 5 Rue de Broglie, 22300 Lannion, France

* Corresponding author: yannick.lecozler@agrocampus-ouest.fr

Abstract

Three-dimensional (3D) imaging is a solution for monitoring morphology and growth of dairy cows, but it can also estimate indicators such as body volume, surface area and body weight. A 3D full-body scanning device was used to scan 64 lactating Holstein cows from March-June 2018. The cows were individually and automatically weighed at a static weighing station (mean ± standard deviation = 673 ± 65 kg). These measured weights were compared to those predicted from regression models based on volume, area or morphological traits determined from 177 3D images. Since some images were truncated due to cow movement or technical problems, we developed additional regression models to reconstruct total volume or area. The accuracy of volume and area measurements was first tested on an inert cylindrical form (coefficients of variation (CVs) < 0.72%). The CVs for repeatability and reproducibility of the method of calculating volume and area from truncated images

were 0.17% and 3.12%, respectively. Cow volume and area ranged from 0.61-0.96 m^3 and 5.80-8.32 m^2 respectively. Five regression models were developed to estimate cow body weight. Their coefficients of determination ranged from 0.82-0.93 with prediction errors of ca. 3% (20 kg) and 4% (29 kg) as a function of volume and area, respectively. The device and the method, evaluated and validated in this study, offer the possibility to use new indicators such as body volume and area in precision livestock farming.

Keywords: volume, area, cows, sensors, 3D images, weight estimation

1. Introduction

New technologies based on image analysis are successfully used to improve management of most types of animal production. They have been developed to detect lameness in cows (van Hertem et al., 2014; Zhao et al., 2018) or to measure body parameters such as body condition score (BCS; Halachmi et al., 2008; Fischer et al., 2015; Sploliansky et al., 2016). Two-dimensional (2D) image approaches used in the past (Marchant et al., 1993; Schofield et al., 1998) were less effective due to the lack of a third dimension, distortion problems, the complexity of calibration and the need for multiple cameras and three-dimensional (3D) reconstruction models. Inexpensive 3D cameras (< 300 €) are now available, which increases the interest in 3D approaches. They have been used to analyze BCS in dairy cattle, using either a fixed (Fischer et al., 2015) or mobile (Kuzuhara et al., 2015) device. Other authors (Negretti et al., 2008; Buranakarl et al., 2012; Guo et al., 2017; Pezzuolo et al., 2018) have also developed and used 3D imaging technologies for a wider variety of livestock. In most cases, animals were measured under laboratory conditions (heavy

equipment and landmarks on animals to guide computer measurements), which provided images of the entire body of restrained animals or portions of the body of unrestrained animals.

Equipment can often be adapted to farm conditions and recent literature describes devices used to estimate body weight (BW) of pigs in barns (Pezzuolo et al., 2018; Wang et al., 2018) and broilers in houses (Mortensen et al., 2016). Inexpensive and portable equipment based on the Microsoft Kinect® v1 sensor have often been used; however, authors concluded that most methods needed additional technical development to acquire and extract data automatically. Using 3D image technology to estimate animal BW is also of interest, since it reduces risky situations for both animals and humans and can provide frequent records. This technology is also suitable for collecting information about animal volume and area. For example, to examine heat stress in an increasingly warm environment, it would be useful to focus on area, since evaporative heat loss in most mammals occurs via perspiration from the skin and respiration (Berman, 2011).

The Morpho3D scanning device was developed to record and monitor morphological traits (Le Cozler et al., 2019). In the present study, we tested the hypothesis that it could also determine volume and area of dairy cows accurately and thus their BW.

2. Materials and methods

2.1. Animals: Data were obtained from the INRA-UMR PEGASE experimental dairy station at Méjusseaume, Le Rheu, in western France (48°11’ N; 1°71’ W; elevation 35 m). The study involved 64 Holstein dairy cows with a mean BW of 673 kg (standard deviation (SD) = 65 kg) and parity ranging from 1-5. After each milking (twice a day), cows were individually and automatically weighed at a static weighing station

(DeLaval France, Elancourt, France) at the milking parlor's exit. Mean BCS, based on the French scoring scale of 0-5 (Bazin et al., 1984), was 2.05 (± 0.25). One month, after weighing, cows were scanned with the Morpho3D device (section 2.3). Data were collected from March-June 2018, yielding 289 3D images. However, due to abnormal behavior of the cows or excessive light in May (which generated artifacts on images), cloud points were considered of too low quality to be used for 3D images reconstruction (Fig.1). As a result, only 177 3D images were used to estimate morphological traits, volume and area.

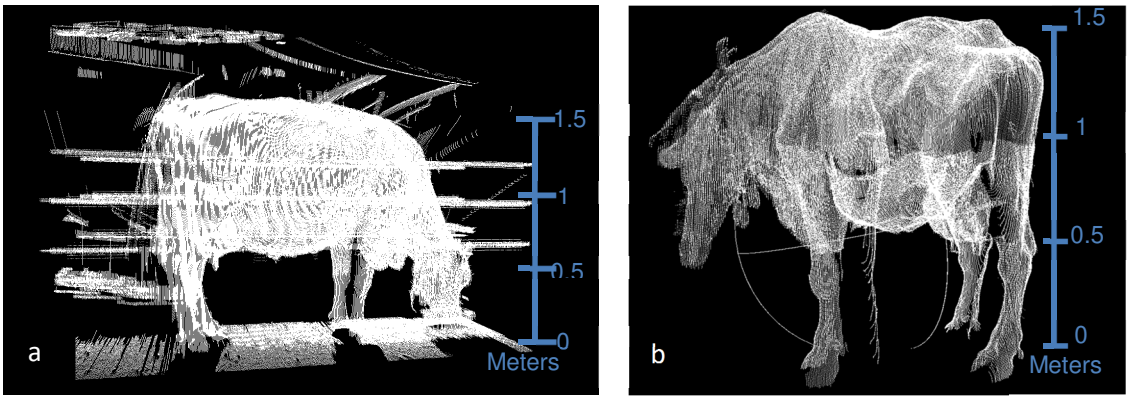

Figure 1. Examples of poor quality cloud points due to (a) excessive light or (b) animal movement.

To limit image quality problems due to animal movements and excess light, the Morpho3D device was then partially covered with an opaque tarpaulin and the installation of a feed fence limited the cow movement.

2.2. Cylinder model: A cylinder model, on which measurements could be performed easily and precisely, was scanned to determine the accuracy of measurements and calculations of volumes and areas from 3D images. The cylinder model was considered the reference object, and its volume and area were measured manually and calculated.

2.3. Morphological acquisition system: 3D images of the cows were acquired automatically using Morpho3D, a sliding acquisition system, located near the weighing station (Fig. 2). Briefly, the system had five cameras, each paired with a laser projector. The VGA image resolution of each camera was 640 × 480 pixels. Two cameras were fixed at 0.40 and 1.77 m above ground level, respectively, on each side of the portal. The fifth camera was fixed to the middle of the top of the portal (3.00 m above ground level). The portal moved at a mean speed of 0.5 $m.s^{-1}$ from back to front (phase 1) and returned to its initial position at a mean speed of 0.3 $m.s^{-1}$ (phase 2). Each camera took 80 images per second only during phase 1, yielding a total of 2,000 images. The cameras were attached to the sliding portal (l = 5.00 m; w = 2.58 m; h = 3.00 m; Fig. 2). See Le Cozler et al. (2019) for additional details about Morpho3D.

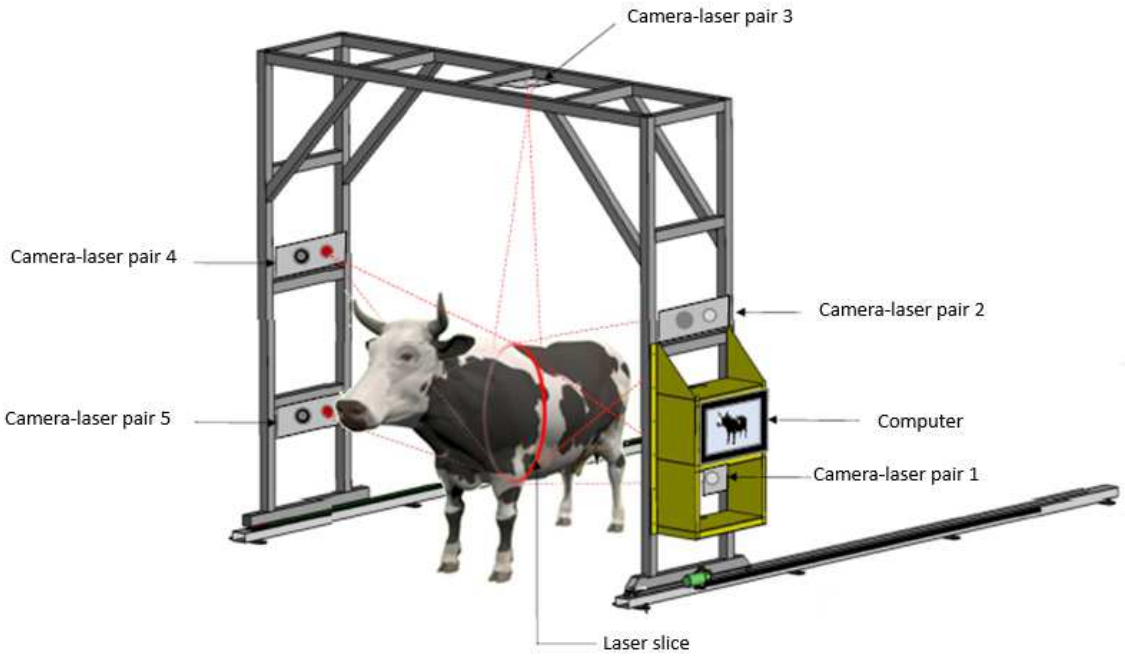

Figure 2. Design of the Morpho3D scanner

Reconstructing an animal in 3D is a generalization of laser triangulation. Each Morpho3D laser generates a vertical plane, whose intersection with the object

appears as a stripe in each image, yielding more points per image. Knowing the equation of the plane in the camera frame allows the 3D position of the points in each stripe in the camera frame to be determined by intersecting the plane with the ray passing through the origin of the camera and the points observed in the image plane. Sliding the system's portal horizontally scans the laser plane over the entire object, yielding a point cloud consisting of several "slices" of 3D points (1 slice = 1 image). These point slices are aggregated based on the location of the system's portal. The cameras were calibrated using a black-and-white checkerboard placed in different locations in the Morpho3D device. Each camera-laser pair was calibrated individually and then two-by-two to calibrate all five cameras collectively. Images of the laser stripes projected onto the cow were captured by their corresponding camera and sent to a computer to reconstruct the cows' 3D information. First, images from each camera were processed to build separate point clouds using calibration information and the speed of the portal. A 3D reconstruction of the entire cow was generated by recording and merging the multiple 3D point clouds from the five camera-laser pairs. This resulted in a single point cloud representation of the entire cow.

Two camera filters were used during image capture: a physical filter centered on the laser wavelength to reduce ambient light and increase the contrast of laser stripes in each image and a software filter to prevent recording of undesirable points too far from the camera. Undesired objects were deleted during a cleaning process using Metrux2α® software (3D Ouest, Lannion, France). This step ensured that the point cloud is a sampling of a smooth surface on which surface normal vectors can be estimated. Finally, surface normals were estimated from the point cloud, and a screened Poisson surface-reconstruction algorithm was applied to build a triangulated mesh (Kazhdan and Hoppe, 2013) using Meshlab® open-source

138 software (Cignoni et al., 2008).

139

140 **2.4. Calculating volume and area**

141 **2.4.1. Principles of calculating volume and area**

142 Metrux2α® was used to perform linear measurements and estimate morphological
143 traits, volume and area. Le Cozler et al. (2019) describe the linear measurements
144 and their validation. Volume and area were automatically calculated by algorithms
145 integrated into Metrux2α®, similar to the method used for morphological traits. Area
146 was calculated from a triangular 3D mesh created from a list of interconnected 3D
147 vertices. Each vertex shared by several triangles was then indexed to identify its
148 position in relation to the other vertices to create a list of triplets of vertices that form
149 the triangles. From this list, the area of each triangle was calculated. The total area of
150 the cow equaled the sum of the areas of the triangles of the 3D mesh.
151 Volume was calculated using the method of Mirtich (1996), based on divergence
152 theorem and Green's theorem. In it, volume equals the volumetric integral of the
153 characteristic function of the object, but this integral cannot be calculated directly for
154 a complex volume. Instead, faces and points, from which calculations can be made,
155 must be introduced. The divergence theorem transforms an integral of the volume
156 into an integral of the area, as follows

157 $$\int_v \nabla . F \, dV = \int_{\delta v} F . \hat{n} \, dA$$

158 where v is the volume, δv is the surface around the volume, ∇ is the nabla operator
159 which characterizes the divergence, F is the vector field of the volume and n is the
160 normal to the surface oriented towards the outside.
161 This divergence theorem is used on a vector field whose divergence is equal to 1 in
162 order to find the characteristic function of the object. In a second step, the surface

around the volume is calculated using Green's theorem, which transforms the integral of the area of the triangles of the 3D mesh into an integral of the segments, themselves calculated from the 2D coordinates of the vertices. This step requires transforming the 3D coordinates into local 2D coordinates. The volume and area of the 3D image are then calculated from the vertices of the triangular 3D mesh.

2.4.2. Application to the cylinder model

We first applied the method to calculate the volume and area of the cylinder model. After scanning, image acquisition and cleaning, a single point-cloud representation of the cylinder was obtained and a triangulated mesh was built (Fig. 3). This process was repeated 10 times to acquire 10 images. We then compared the volumes and areas calculated by Metrux2α® to those calculated by Meshlab®, since the latter is widely used for this purpose. We also compared the volume and area measured manually to those calculated by Metrux2α®.

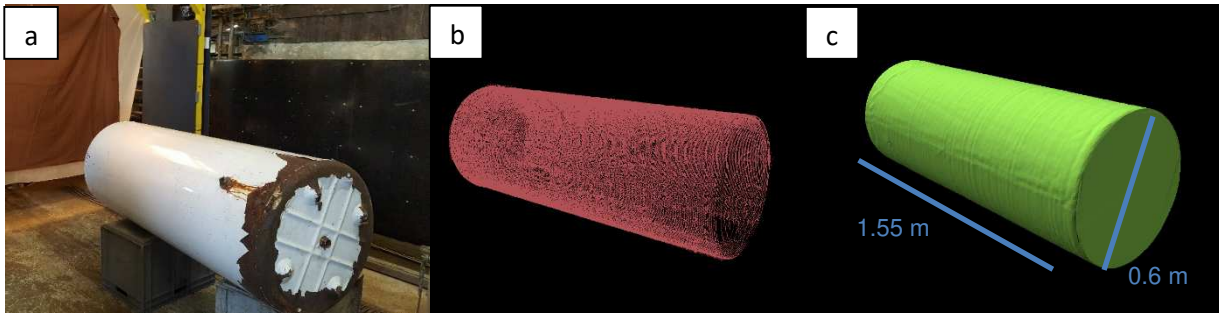

Figure 3. Data acquisition from (a) the reference cylinder model (b) the raw point cloud after cleaning and (c) the final 3D image after Poisson surface-reconstruction.

2.4.3. Application to living animals

Due to animal movement, not all images could be used in full. Although the cow's body was digitized properly, its head usually moved, which sometimes distorted its

184 volume and area. It was sometimes necessary to restrain younger and/or nervous
185 animals in a feed fence during image acquisition. As a result, the image was cut off at
186 shoulder level (Fig. 4).
187

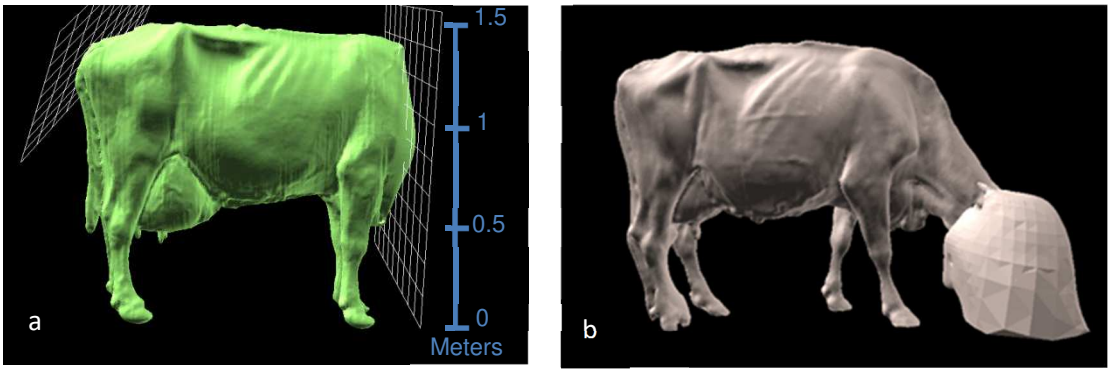

188 Figure 4. Images obtained when a cow was (a) restricted in a feeding fence (truncated
189 image) or (b) its head moved too much during image acquisition.
190

191 To decrease cow movement without affecting the lasers, we provided concentrate
192 feed in a rectangular bowl, either opaque plastic or transparent glass. The presence
193 of the opaque plastic bowl changed the shape of the cow's volume (Fig. 5). The
194 depth of the cow's head in the bowl at the time of acquisition varied, but the addition
195 of the bowl to the cow's head added a maximum volume of 5 dm^3 and area of ca. 0.2
196 m^2 (Fig. 5a). In some images, the bowl truncated the head, removing a mean volume
197 of 3 dm^3 and a mean area of 0.1 m^2 (Fig. 5b). To avoid this bias, the transparent
198 glass bowl was used, which did not distort the cow's head, allowing volume and area
199 of the cow to be calculated accurately (Fig. 5c).
200
201
202
203

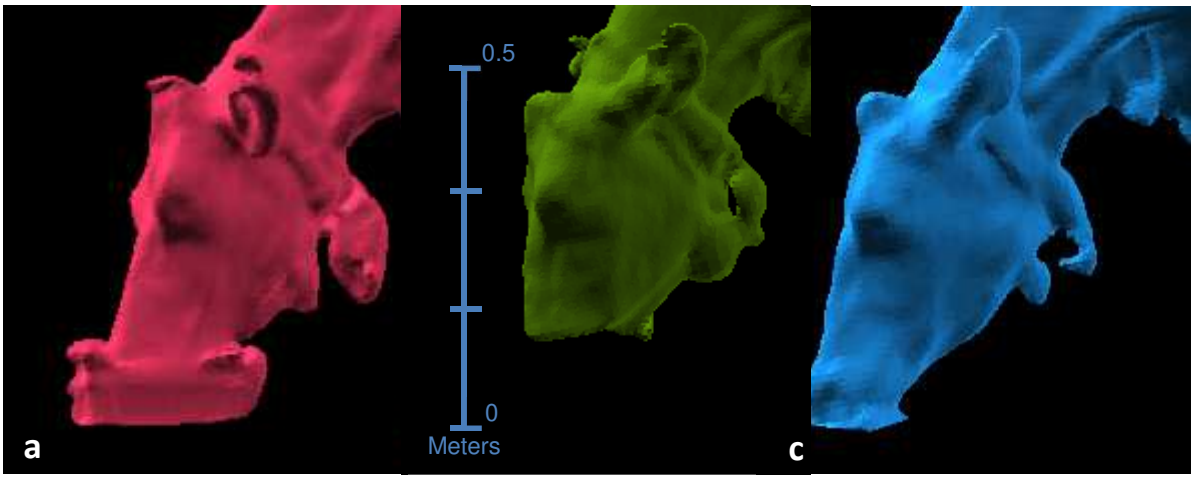

Figure 5. Differences in cow head reconstruction with (a) an opaque plastic bowl, (b) an opaque plastic bowl that truncates the head or (c) a transparent glass bowl.

Given the need to restrain some cows, we assessed the ability to estimate total volume and area from images of animals cut off at shoulder level. Only high-quality images (i.e. with the head scanned correctly) were selected. Two volumes and areas were determined on from the images: total volume and area, calculated using the automatic algorithm, and truncated volume and area, measured by placing one plane at the tip of the shoulder blades (similar to that used by Minagawa (1994)) and another at the rump (Fig. 6).

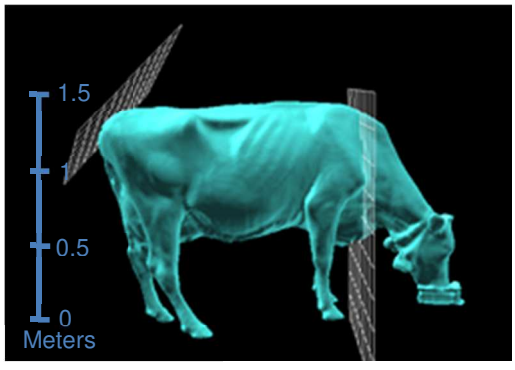

Figure 6. Position of the cutting planes used to estimate truncated volume and area when the head was missing from an image (i.e. cow restrained by a feed fence)

225 The two planes were placed using 3D image-processing software Metrux2α® after
226 placing three points on the image (Fig. 5). The Metrux2α® was used to estimate the
227 volume and area between the two planes and to measure six morphological traits
228 from the images: heart girth, chest depth, wither height, hip width, backside width and
229 ischial width. Details of these traits are available in Le Cozler et al. (2019).
230 Area and volume could be influenced by surface noise and some apparent
231 roughness. Cleaning the resulting points cloud before creating the image required
232 then patience and precision. Nevertheless, for some images, the reconstruction was
233 sometimes not totally satisfactory (e. g. tail stuck to the animal, which was not the
234 case on points cloud). But these errors were finally negligible, since the validation
235 tests, carried out on different images of the same animals showed extremely small
236 variations (see section 3.3)."
237
238 **2.5. Repeatability and reproducibility analyses**
239 As done for morphological traits (Le Cozler et al., 2019), we used the Morpho3D
240 device to estimate the repeatability and reproducibility of calculating volume and
241 area.
242
243 **2.5.1. Repeatability and reproducibility of plane placement**
244 Since total volume and area were calculated automatically, their repeatability and
245 reproducibility did not require assessment (i.e. no variation among measurements
246 due to the operator). For truncated images, however, the repeatability of plane
247 placement and point identification was analyzed to determine whether, for a given
248 image, the placement of planes was reliable and whether the same volume or area
249 could be calculated. Five images of complete cows were used, on which the same

operator placed the cutting planes five times. Truncated volume and area were thus calculated five times from each of five different images.

For reproducibility, we assessed the ability of different operators to identify visually where to place the cutting planes. On images of five cows scanned only once, two operators repeated the placements five times each. In total, we assessed 50 measurements (25 per operator) on five different images. Truncated volume and area were then calculated.

2.5.2. Reproducibility of volume and area of the Mopho3D device in a changing environment

Analysis of reproducibility aimed to verify whether the method was able to calculate the same values from different image acquisitions in a changing environment caused by variability in cow position, image reconstruction and operator plane placements. Reproducibility was assessed using images of nine cows, each undergoing the entire procedure, from initial acquisition to calculation of volume and area, five times. The same operator performed all of the manipulations. In this procedure, the reproducibility combined the repeatability error of volume and area calculation with that of plane placement.

2.5.3. Calculation

Variability in volume and area calculated from the 3D images was corrected for the effect of individual cows by extracting residuals from an analysis of variance (ANOVA) model. Repeatability and reproducibility were estimated using the SDs of placement repeatability (σ_{rp}), inter-operator reproducibility (σ_{Ro}) and reproducibility in a changing environment (σ_{Ri}). Values of σ_{rp} and σ_{Ri} were calculated from the residues

of the single-factor ANOVA of the individual-cow effect, while σ_{Ro} was calculated from the mean of the reproducibility SDs of an ANOVA of the operator effect. Existing variations among cows were then excluded from the analysis. The coefficients of variation of repeatability (CV_{rp}) and those of inter-operator and changing environment reproducibility (CV_{Ro} and CV_{Ri}, respectively) were then estimated from their respective means (μ_{rp}, μ_{Ro} and μ_{Ri}, respectively) and SDs (σ_{rp}, σ_{Ro} and σ_{Ri}, respectively). The more repeatable (or reproducible) the 3D measurement, the smaller was its CV_{rp} (or CV_{Ro} or CV_{Ri}).

2.6. Estimation of body weight

Cow BW was measured twice a day. BW was also predicted using several regression models based on morphological traits, volume and area calculated with the Morpho3D device. Predictions of these models were then compared to the BW measured with the weighing system. From the measurements performed on complete images, a correlation matrix of Pearson coefficients was calculated to identify relationships between traits. Volume, area and morphological traits were measured or/ calculated from 3D images, while other traits, such as BCS and BW, were available in the database of the herd management system.

Several linear regression models to predict BW from traits measured or calculated from the 3D images were tested. The models were developed using the Akaike information criterion (AIC) with "backward elimination" variable selection. This method begins with all variables and then removes one or more variables at each iteration until it obtains the minimum value of the AIC, defined as $2 \times (n-2) \times \log(L)$, where n is the number of variables in the model and L is the maximum probability of the likelihood function. Each final model was cross-validated to estimate its prediction

error. Cross-validation was preferred due to the small size of the dataset, which precluded separating it into sufficiently large calibration and validation datasets. The dataset was thus randomly divided into 2 groups, one of them containing 90%of datasets. This large group was used to develop BW models, which were then validated on data from the remaining group. Ten iterations of each model were cross-validated 100 times using different random draws to obtain a large number of variations and calculate the root mean square error of prediction (RMSEP). Coefficient of determination (R^2) and RMSEP of the models were calculated to determine the quality of the linear regression and quantify the mean prediction error made by the model during cross-validation, respectively.

2.7. From truncated to complete images

Total volume and area were predicted using regression models based on truncated images. As before, models were developed using AIC with "backward elimination" variable selection. The same variables, except for total volume and area, were used in the models. Two models for each variable (total volume and total area) were developed: one with multiple variables that minimized RMSEP and another with only truncated area or volume. As before, 10 iterations of each model were cross-validated 100 times using different random draws to obtain a large number of variations and calculate RMSEP.

2.8. Statistical analysis

All statistical analyses (i.e. ANOVA, repeatability, reproducibility, correlation analysis) were performed using R software (R Core Team, 2016).

3. Results

3.1. Volume and area of the cylinder model

The error in determining both volume and area of the cylinder model was 0.0005% for Metrux2α® and 0.0001% for Meshlab®. Differences between Metrux2α® estimates and manual measurements were less than 1%, regardless of the trait (Table 1).

Table 1. Mean and standard deviations (SD) of traits of the cylinder model estimated by the Morpho3D device (10 images) and absolute and relative differences between them and manual measurements.

Trait	Mean	SD	Difference	
			Absolute	Relative
Length (h), m	1.552	0.010	-0.010	0.62%
Circumference (d x π), m	1.880	0.005	-0.008	0.24%
Surface area (π x d x (h + d/2)), m^2	3.490	0.015	-0.028	0.44%
Volume (π x $(d/2)^2$ x h), m^3	0.440	0.003	-0.003	0.72%

3.2. Volume and area of cows

Morphological traits, volume and area were measured or calculated for the 64 Holstein dairy cows (Table 2). Mean (± 1 SD) volume and area of cows was 0.76 (± 0.07) m^3 and 6.84 (± 0.45) m^2, respectively. Truncated volume and area equaled 90% and 81% of total volume and area, respectively. Density of the cows (i.e. BW/total volume) was 0.89 kg dm^{-3}, but ranged 0.79 to 0.95 kg dm^{-3}.

Table 2. Mean, standard deviation (SD), and minimum and maximum values of body weight, body condition score (French scale of 0-5 (Bazin et al., 1984)), morphology, volume and area of 64 dairy Holstein cows measured or calculated from 177 images. Truncated volume and area were calculated from the tip of the shoulder blades to the rump by placing one plane at each location.

Body trait	Mean	SD	Min.	Max.
Body weight, kg	673	65	539	871
Body condition score	2.05	0.25	1.50	2.88
Heart girth, cm	228	10	210	256
Chest depth, cm	85.9	3.2	78.8	95.3
Wither height, cm	146	5	135	160
Hip width, cm	58.8	3.4	50.7	66.7
Backside width, cm	53.8	2.7	44.3	63.5
Total volume, m^3	0.76	0.07	0.61	0.96
Truncated volume, m^3	0.69	0.07	0.56	0.84
Total area, m^2	6.84	0.45	5.80	8.32
Truncated area, m^2	5.53	0.39	4.60	7.17
Density, kg dm^{-3}	0.89	0.03	0.79	0.95

3.3. Reproducibility and repeatability

Repeatability estimated the error related to an operator's placement of planes on truncated images. Placement of the planes varied little (σ_{rp} for volume and area = 0.17% and 0.32%, respectively). Inter-operator reproducibility had larger error, σ_{Ro} for volume and area 1.00% and 1.80%, respectively. Reproducibility of total and

truncated values in a changing environment (σ_{Ri}) had even higher errors (CVs for both = ca. 2-3%) (Table 3). In calculations of total volume and area, CVs expressed measurement error related to image acquisition and processing. In calculations of truncated volume and area, CVs combined image acquisition and processing error with plane-placement error.

Table 3. Reproducibility of total and truncated volume and area in a changing environment assessed by standard deviation (SD) and coefficient of variation (CV). Truncated volume and area were calculated from the tip of the shoulder blades to the rump by placing one plane at each location.

Repeatability	Mean	SD	CV
Total volume, m^3	0.78	0.02	2.24%
Truncated volume, m^3	0.72	0.02	2.43%
Total area, m^2	6.94	0.02	2.85%
Truncated area, m^2	5.59	0.1	3.12%

3.4. Estimating body weight from 3D images

Traits measured from 3D images were strongly correlated with each other and with BW (Table 4). BCS was not correlated with other variables (maximum r = 0.22). BW and volume (total or truncated) were strongly correlated (r = 0.93 and 0.92, respectively). Volume and area (total or truncated) were also strongly correlated (r = 0.84-0.87).

372 Table 4. Correlation matrix between traits measured and/or estimated from 3D images. Truncated volume and area were calculated from the tip
373 of the shoulder blades to the rump by placing one plane at each location. (Under the diagonal: Pearson correlation coefficient; Above the
374 diagonal: p-value of the correlation). BCS: body condition score, BW: body weight.

Trait	Total volume	Truncated volume	Total area	Truncated area	Hip width	Wither height	Chest depth	Heart girth	Backside width	BCS	BW
Total volume	-	*<0.001*	*<0.001*	*<0.001*	*<0.001*	*0.012*	*0.296*	*0.502*	*0.008*	*0.020*	*<0.001*
Truncated volume	0.99	-	*<0.001*	*<0.001*	*<0.001*	*0.012*	*0.298*	*0.535*	*0.008*	*0.018*	*<0.001*
Total area	0.87	0.86	-	*<0.001*	*0.004*	*0.017*	*0.407*	*0.948*	*0.025*	*0.007*	*0.003*
Truncated area	0.84	0.86	0.94	-	*0.005*	*0.019*	*0.485*	*0.871*	*0.027*	*0.010*	*0.004*
Hip width	0.76	0.76	0.64	0.62	-	*0.010*	*0.221*	*0.537*	*0.002*	*0.002*	*<0.001*
Wither height	0.66	0.66	0.62	0.61	0.61	-	*0.008*	*0.435*	*0.191*	*0.020*	*0.007*
Chest depth	0.56	0.56	0.50	0.45	0.52	0.67	-	*0.083*	*0.934*	*0.318*	*0.152*
Heart girth	0.54	0.53	0.40	0.31	0.44	0.43	0.56	-	*0.824*	*0.718*	*0.334*
Backside width	0.61	0.61	0.53	0.50	0.61	0.38	0.30	0.26	-	*0.001*	*0.004*
BCS	0.15	0.14	0.04	0.01	-0.03	0.05	0.20	0.22	-0.12	-	*0.031*
BW	0.93	0.92	0.72	0.71	0.80	0.70	0.63	0.57	0.66	0.19	-

375

Since correlations between BW and the main traits were linear, linear regression models (1) and (2) were developed with the maximum number of variables from complete images using AIC (Table 5). After testing these more complex models, we included only 1-3 variables in models (3) and (4).

Table 5. Models predicting body weight (BW, in kg) of cows as a function of selected traits measured from complete images from the Morpho3D device. Model quality was assessed with a coefficient of determination (R^2) and root mean square error of prediction (RMSEP).

Model		BW		
		R^2	RMSEP	
(1)	$BW = 812.1 \times total\ volume - 81.4 \times area + 343.8 \times backside\ width + 273.8 \times hip\ width + 208.8 \times heart\ girth + 113.7 \times wither\ height - 280.7$	0.93	18.2	2.72%
(2)	$BW = 31{,}7 \times area + 608.8 \times hip\ width + 593.4 \times backside\ width + 257.2 \times wither\ height + 152.8 \times heart\ girth - 905.3$	0.82	29.3	4.38%
(3)	$BW = 620 \times total\ volume + 379 \times backside\ width + 287\gamma \times hip\ width - 174$	0.88	22.5	3.36%
(4)	$BW = 827.5 \times total\ volume + 45.8$	0.85	24.9	3.72%
(5)	$BW = 102.3 \times total\ area - 30.33$	0.49	45.2	8.75%

For the selected traits, see corresponding units in tables 3 and 4

Model (1) was the most accurate (RMSEP = 2.72%, R^2 = 0.93); it included six of nine possible traits (BCS not included because of the lack of correlation) previously mentioned): total volume, total area, hip width, backside width, wither height and chest depth. However, the coefficient of collinearity between total volume and total area was greater than 4 (not presented). Other models, free of strong collinearity and therefore more generalizable, were tested, such as including area but not volume (model (2)), or volume but not area (model (3)), but they were less accurate (RMSEP = 3.36% and 4.70%, respectively). A 4th model, which considered only volume, was only moderately accurate (R^2 = 0.85, RMSEP = 3.72%), which corresponded to an

error of 25 kg in predicted BW. In a similar way, a final model (5), which considered only area, indicated a poor accuracy (R^2 = 0.49, RMSEP = 6.75%), which corresponded to an error of 45 kg in predicted BW.

3.5. Predicting total volume and area from truncated images

Since it was not always possible to acquire complete images, total cow volume and area were predicted from truncated images (Table 6). A model using only truncated volume (model (5b) predicted total volume accurately (R^2=0.98, RMSEP = 1.05%), and adding heart girth increased its accuracy (model (5a), R^2 = 0.99, RMSEP = 1.02%). A model using only truncated area predicted total area accurately (model (6b), R^2 = 0.85, RMSEP = 2.22%), and adding heart girth and backside width increased its accuracy (model (6a), R^2 = 0.90, RMSEP = 2.14%); however, it was still less accurate than the prediction of total volume.

Table 6. Models estimating total volume or total area of cows from truncated images. Model quality was assessed with a coefficient of determination (R^2) and root mean square error of prediction (RMSEP). Truncated volume and area were calculated from the tip of the shoulder blades to the rump by placing one plane at each location.

Model		R^2	RMSEP	
(5a)	$Total\ volume\ = 1.0595 \times truncated\ volume\ + 0.0165 \times heart\ girth\ - 0.0149$	0.99	0.008	1.02%
(5b)	$Total\ volume\ = 1.0704 \times\ volume + 0.0154$	0.98	0.008	1.05%
(6a)	$Total\ area\ =\ 0.990 \times truncated\ area + 1.039 \times backside\ width + 0.518 \times heart\ girth - 0.365$	0.90	0.146	2.14%
(6b)	$Total\ area\ =\ 1.07 \times truncated\ area + 0.94$	0.85	0.152	2.22%

For the selected traits, see corresponding units in tables 3 and 4

4. Discussion

Scanning an inert cylinder showed that the scanner could accurately acquire and calculate volume, area, length and circumference with less than 1% error. The validation process assessed image acquisition and processing and thus validated the overall accuracy of the method. This method can calculate volume and area with high reproducibility (CV = 2.24% and 2.43%, respectively). On living animals, the reproducibility coefficients for calculating volume and area were slightly higher due to manual manipulation (placement of planes) and were quantified by the repeatability of the placement of planes (0.17% and 0.32% for volume and area, respectively). A future study could calculate the repeatability and reproducibility of each step of the method to identify when the method becomes less accurate.

To assess the interest of developing this tool to render measurements automatic or semi-automatic, inter-operator reproducibility of plane placement was considered high (CVs for volume and area measurement = 1.00% and 1.80%, respectively). According to Fischer et al. (2015), a method is repeatable and reproducible when its CV is less than 3-5%. Unfortunately, repeatability and reproducibility tests are not widely available in the literature, even though they are essential for determining the relevance of tools and methods (Marinello et al., 2015). It is therefore difficult to compare the method we developed to other tools.

The model used most often to estimate body area was developed by Mitchell (1928): $0.14 \times BW^{0.67}$. Other models are also available ((Elting 1926): (a): $0.147 \times BW^{0.56}$, (b): $0.0839 \times BW^{0.67}$; Brody (1945): $0.14 \times BW^{0.57}$; Johnson et al., (1961): $0.235 \times BW^{0.46}$). When we applied these models to the recorded BW in our database, some

yielded lower BW (Elting, 1926, model a; Brody, 1945; Johnson et al., 1961), similar BW (Elting et al., 1926, model b; Mitchell, 1928) or higher BW (Meeh, 1879) (Fig. 6).

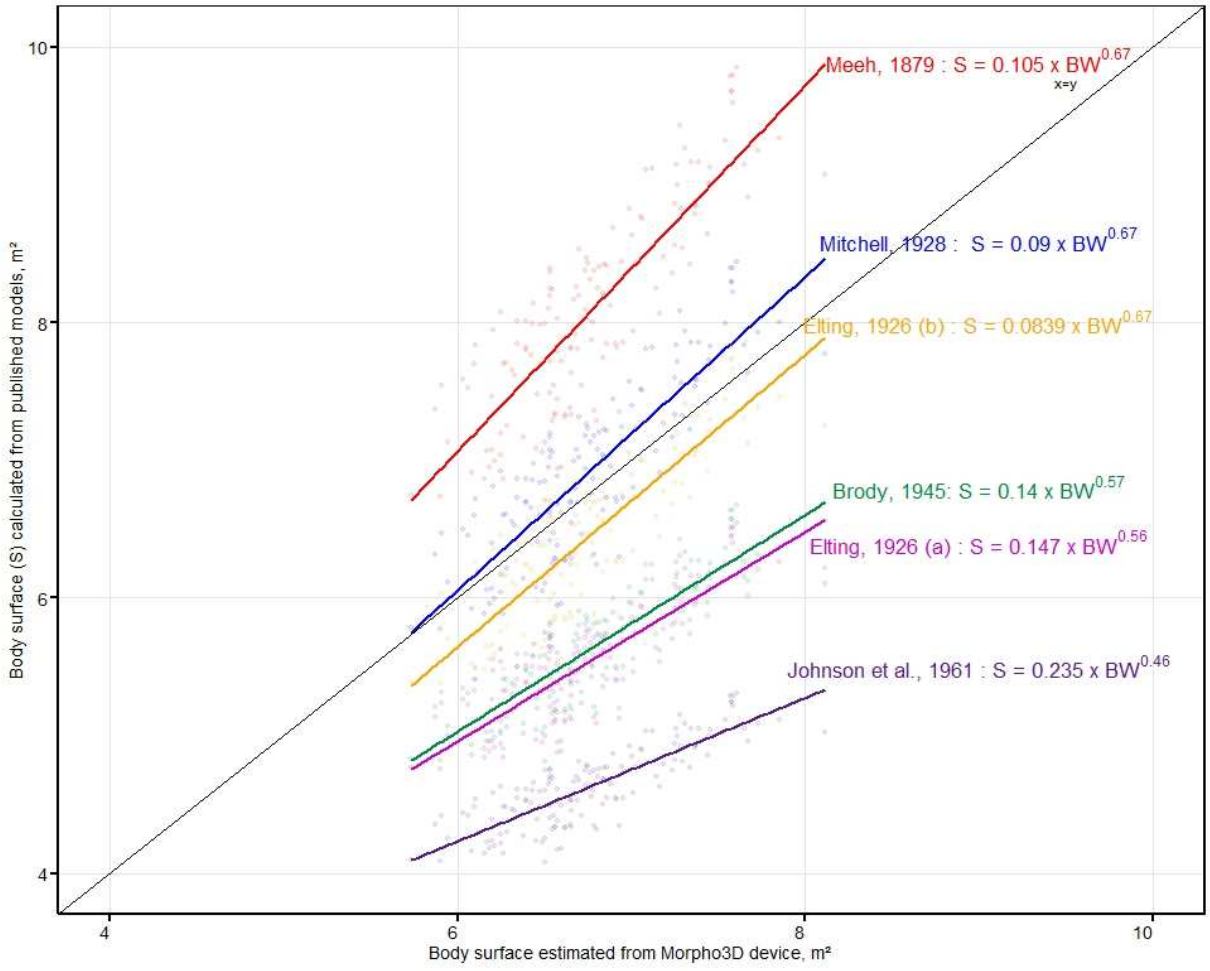

Figure 6. Surface area of cows predicted by published models *vs*. those calculated using the Morpho3D device.

Errors resulting from the image-reconstruction process or low-quality images may occur with the Morpho3D device. Other methods that estimate area, however, also have limits and can be difficult to use (e.g. the model of Mitchell (1928)). Future studies that accurately estimate area are needed with other methods than with Morpho3D device, but access to a large number of animals could be challenging, as well as determining arear with such methods

Like for body area, little information is available on cow volume. Minagawa (1994) estimated the volume of the neck and head of beef cows, and the results indicated that the rest of the body's volume was similar to our truncated volume. By applying our model (5b, Table 6) to this truncated volume, we predicted less than 1.5% difference in the total volume for four of Minagawa's five cows. The difference in total area was less than 6%.

Validating the methods used to estimate morphological traits, volume and area from 3D images enabled us to use these data to estimate cow BW, which is useful in breeding and feeding programs, commercial transactions and in the search for new indicators to estimate food-use efficiency in dairy animals. Estimation of BW, particularly during the rearing period, has been based for decades on development indicators (Heinrichs et al., 1992). It is indeed traditionally and commonly used in livestock production to follow growth of animals and/or then, adapt their feeding regimes. It is also used for commercialisation purposes for examples. Most feeding regimes for ruminants, pigs or poultry are based on animal body weight, which is rarely measured on-farms. As a result, recommendations are often based on visual estimation of BW. In addition, when performed so far, BW measurements are done manually, using weighing systems, which are also time consuming, sometimes costly, risky for human and animals health. Methods to estimate BW based on image technologies are then of increasing interest for many research groups, breeding organization, farmers and advisors. Estimating animal BW from measurements made from 3D images is a recent possibility (Anglart, 2010; Buranakarl et al., 2012; Kuzuhara et al., 2015). Anglart (2010) applied this approach to 3D acquisition of the

backs of Holstein dairy cows using a time-of-flight camera, obtaining a R^2 for BW of 0.87. Of the 6224 acquisitions, however, 30% of the BW estimated from the images had an error of more than 30 kg. Buranakarl et al. (2012) acquired full-body 3D images of buffaloes and developed 12 BW prediction equations (four each for all buffaloes, females and males) by changing the number of parameters considered. For females, they obtained an R^2 for BW of 0.89 using four parameters (wither height, shoulder width, ischial width, length from ischia to shoulders). Kuzuhara et al. (2015) predicted BW from seven traits (RMSEP = 42 kg). The models used in the present study were therefore satisfactory (R^2 = 0.82-0.93, RMSEP from 2.72% (18.2 kg) to 4.38% (29.3 kg)) compared to those previously published. Since only 16% of the BW had an error greater than 30 kg (model (3)), the scanner and the method used appear reliable. Unlike previous studies that used only linear traits as parameters, 3D imaging can create new models using volume and area. Ultimately, 3D imaging enables accurate and simplified estimation of BW from the traits measured, especially because it allows calculation of volume, which is strongly correlated with BW. Nevertheless, more automation (e.g. image preparation and measurement) is required to fully benefit from this tool.

Conclusion and future studies

The scanning technology described in this study provides new perspectives for assessing animal morphology and can be used to calculate volume and area of dairy cows. Analyses indicated that it was possible to estimate total volume and area from truncated images; however, all images had the same degree of truncation. Future studies are needed to determine whether other cutting planes (i.e. types of other types of truncation) could be useful. This suggests that truncated images from a less

503 complicated or portable device could be used in the future. In addition, the device
504 can also be used to estimate BW which is useful information, without investing in a
505 weighing system. Preliminary results also indicated that the device can estimate
506 changes in volume in the short term (rumen content), medium term (embryo
507 development) and long term (growth).
508 The Morpho3D device allowed the acquisition of new phenotypes, not accessible
509 until now, such as area and volume, at high-flow rates. There were no plans to
510 implement this device on a large scale in commercial farms. For this purpose, a new
511 version, not depending on animal movements and not sensitive to ambient light, is
512 being tested. The quality of the 3D-images is lower, but sufficient to estimate most
513 parameters previously presented, that will be compared to values obtained from
514 Morpho3D device, considered as "Gold Standards".
515

516 **Acknowledgments**

517 The authors wish to thank everyone involved in the Morpho3D project, especially
518 technicians at the Méjusseaume experimental station, who took excellent care of the
519 animals. The Morpho3D project is supported by the National Fund CASDAR, which
520 supports innovation in agriculture (RFP “Recherche Technologique” 2015, no. 005),
521 special funds from the INRA Animal Physiology and Livestock Systems division for
522 innovative projects and the collaborative ANR – APIS-GENE project DEFFILAIT.
523

524 **References**

525 Anglart, D., 2010. Automatic estimation of body weight and body condition score in dairy cows using
526 3D imaging technique. Swedish University of Agricultural Sciences, Master’s thesis.
527 Bazin, S., Augeard, P., Carteau, M., Champion, H., Chilliard, Y., Cuylle, G., Disenhaus, C., Durand,G.,
528 Espinasse, R., Gascoin, A., Godineau, M., Jouanne, D., Ollivier, O., Remond, B., 1984. Grille de

notation de l'état d'engraissement des vaches pie-noires. Institut Technique de l'Elevage Bovin, Paris, France.

Berman, A., 2003. Effects of body surface area estimates on predicted energy requirements and heat stress. Journal of Dairy Science 86, 3605-3610.

Buranakarl, C., Indramangala, J., Koobkaew, K., Sanghuayphrai, N., Sanpote, J., Tanprasert, C., Phatrapornnant, T., Sukhumavasi, W., Nampimoon, P., 2012. Estimation of body weight and body surface area in swamp buffaloes using visual image analysis. Journal of Buffalo Science, 1, 13-20.

Cignoni, P., Callieri, M., Corsini, M., Dellepiane, M., Ganovelli, F. Ranzuglia, G., 2008. MeshLab: an Open-Source Mesh Processing Tool. Sixth Eurographics Italian Chapter Conference, 129-136.

Elting, E.C., 1926. A formula for estimating surface area of dairy cattle. Journal of Agriculture Research 33, 3, 269-279.

Fischer, A., Luginbuhl, T., Delattre, L., Delouard, J. M., Faverdin, P., 2015. Rear shape in 3 dimensions summarized by principal component analysis is a good predictor of body condition score in Holstein dairy cows. Journal of Dairy Science 98, 4465 - 4476.

Guo H., Ma, X., Ma, Q., Wang, K., Su, W., Zhu D., 2017. LSSA_CAU: an interactive 3d point clouds analysis software for body measurement of livestock with similar forms of cows and pigs. Computers and Electronics in Agriculture, 138, 60-68.

Halachmi, I., Polak, P., Roberts, D.J., Klopcic, M., 2008. Cow body shape and automation of condition scoring. Journal of Dairy Science, 91, 4444-4451.

Heinrichs, A.J., Rogers, G.W., Cooper, J.B., 1992. Predicting body weight and wither height in Holstein heifers using body measurements. Journal of Dairy Science, 75 (12), 3576-3581.

Kazhdan, M., Hoppe, H., 2013. Screened Poisson surface reconstruction. ACM Transactions on Graphics, 32 (3), Article 29.

Kuzuhara, Y., Kawamura, K., Yoshitoshi, R., Tamaki, T., Sugai, S., Ikegami, M., Kurokawa, Y., Obitsu, T., Okita, M., Sugino, T., Yasuda, T., 2015. A preliminarily study for predicting body weight and milk properties in lactating Holstein cows using a three-dimensional camera system. Computers and Electronics in Agriculture, 111, 186-193.

Le Cozler Y, Allain A, Caillot A, Delouard JM, Delattre L, Luginbuhl T, Faverdin P 2019. High precision scanning system for complete 3D cow body shape imaging and analyzing morphological traits. Computers and electronics in Agriculture 157,447-453.

559 Marchant, J.A., Schofield, C.P., 1993. Extending the snake image processing algorithm for outlining
560 pigs in scenes. Computers and Electronics in Agriculture, 8, 261-275.
561 Minagawa, H., 1994. Surface area, volume, and projected area of Japanese-shorthorn cattle
562 measured by stereo photogrammetry using non-metric cameras. Journal of Agriculture Met 50(1),
563 17-22.
564 Mirtich, B., 1996. Fast and accurate computation of polyhedral mass properties. Journal of Graphics
565 Tools 1 (2), 31-50.
566 Mortensen, A.K., Lisouski, P., Ahrendt, P., 2016. Weight prediction of broiler chickens using 3D
567 computer vision. Computers and Electronics in Agriculture, 123, 319-326.
568 Negretti, P., Bianconi, G., Bartocci, S., Terramoccia, S., Verna, M., 2008. Determination of live weight
569 and body condition score in lactating Mediterranean buffalo by Visual Image Analysis. Livestock
570 Science, 113, 1-7.
571 Pezzuolo, A., Guarino, M., Sartori, L., Marinello, F., 2018. A feasibility study on the use of a structured
572 light depth-camera for three-dimensional body measurements of dairy cows in free-stall barns.
573 Sensors, 18, 673, doi: 10.3390/s18020673.
574 Pezzuolo, A, Guarino, M., Dartori, L., Gonzalez, L.A., Marinello, F., 2018. On-barn pig weight
575 estimation based on body measurements by a Kinect v1 depth camera. Computers and Electronics
576 in Agriculture, 148, 29-36.
577 R Core Team 2019. R: a language and environment for statistical computing. R Foundation for
578 Statistical Computing, Vienna, Austria. Version 3.2.4. Retrieved 1 April 2016 from https:// www .r-
579 project.org/.
580 Schofield C. P., Marchant J. A., White R. P., Brandl N., Wilson M. 1999. Monitoring of pig growth using
581 prototype imaging system. Journal of Agricultural Engineering Research, 72, 3, 205-210.
582 Spoliansky, R., Edan, Y., Parmet, Y., Halachmi, I., 2016. Development of automatic body condition
583 scoring using a low-cost 3-dimensional Kinect camera. Journal of Dairy Science, 99, 9, 7714 -
584 7723.
585 Van Hertem, T., Viazzi, S., Steensels, M., Maltz, E., Anatler, A., Alchanatis, V., Schlageter-Tello, A.A.,
586 Lokhorst, K., Romanini, E.C.B., Bahr, C., Berckmans, D., Halachmi, I., 2014. Automatic lameness
587 detection based on consecutive 3D-video recordings. Biosystems Engineering, 119, 108-116.

588 Wang, K., Guo, H., Ma, Q., Su, W., Chen, L., Zhu, D., 2018. A portable and automatic Xtion-based
589 measurement system for pig body size. Computers and Electronics in Agriculture, 148, 291-298.
590 Zhao, K., Bewley, J.M., Heade, D., Jin, X., 2018. Automatic lameness detection in dairy cattle based
591 on leg swing analysis with an image processing technique. Computers and Electronics in
592 Agriculture, 148, 226-236.